Electric Dyadic Green's Functions for Modeling Resonance and Coupling Effects in Waveguide-Based Aperture-Coupled Patch Arrays

Alexander B. Yakovlev[1], Sean Ortiz[2], Mete Ozkar[2], Amir Mortazawi[3], and Michael B. Steer[2]
[1]Department of Electrical Engineering, The University of Mississippi, University, MS 38677-1848
[2]Department of Electrical and Computer Engineering, North Carolina State University, Raleigh, NC 27695-7914
[3]Department of Electrical Engineering and Computer Science, University of Michigan, Ann Arbor, MI 48109

Abstract— **An efficient technique for the rapid development of electric Green's dyadics of a transversely layered, terminated rectangular waveguide is presented with application to waveguide-based aperture-coupled patch arrays. This technique uses a partial eigenfunction expansion resulting in a Sturm-Liouville problem for one-dimensional characteristic Green's functions in the waveguiding direction. In this representation, the one-dimensional characteristic Green's functions provide physical insight into resonance and surface wave effects occurring in overmoded layered waveguide transitions. Particularly, this is related to the correlation between transverse resonances in the waveguide cross-section and surface waves associated with a grounded dielectric slab waveguide. This is demonstrated for the examples of aperture-coupled patch arrays in the N-port waveguide transition, although the analysis is applicable to other waveguide-based antenna structures, which allow for the propagation of surface waves.**

Index Terms — **Dyadic Green's functions, integral equations, method of moments, patch, slot arrays, waveguide transition, surface waves.**

I. Introduction

The work described here was motivated by the need to develop a modeling environment for waveguide-based spatial power combining circuits in order to increase the general understanding of the system behavior and to aid in the design process. A general algorithm for the analysis of waveguide-based amplifier arrays has been recently developed in [1], [2]. The full-wave analysis of interacting electric- (patch, strip) and magnetic-type (slot, aperture) antennas is based on the Generalized Scattering Matrix (GSM) approach in conjunction with the integral equation formulation for electric and magnetic currents discretized via the Method of Moments (MoM). The electric Green's dyadics in this formulation provide the necessary relationship between scattered fields and induced currents serving as kernels of the integral equations.

Dyadic Green's functions for rectangular waveguides and cavities have been studied by many authors. A traditional and general way to construct Green's functions for a closed-boundary guided-wave structure, semi-infinite waveguide, and cavity is to use the Hansen vector wave functions M, N, and L (or only transverse functions M and N) in a double series expansion [3, p. 1782], [4]. Thus, electric and magnetic dyadic Green's functions for uniform infinite and semi-infinite rectangular waveguides were obtained in [4]–[6], and in [4]–[7] for a rectangular cavity. Also, this type of Green's function expansion was utilized by other authors, for example, in [8] for exterior and interior electromagnetic boundary value problems. There also has been work on dyadic Green's functions for a rectangular waveguide with multilayered dielectric, filled transversely with respect to the direction of wave propagation. Electric and magnetic Green's functions for an infinite waveguide with the transverse dielectric slab were presented in [9] for a full-wave analysis of antenna radiation in a layered rectangular waveguide. The method of mode expansion and scattering superposition were applied in [10] to construct the electric Green's function for a multilayered rectangular waveguide. A general way of constructing electric and magnetic dyadic Green's functions for a multilayered, terminated rectangular waveguide was proposed in [11], where coefficients of Green's functions in a double series expansion were obtained in terms of recurrent transmission matrices.

An alternative representation of a Green's function for closed-boundary cylindrical waveguides and cavities is a series expansion over the complete system of eigenfunctions of a Sturm-Liouville operator with the one-dimensional characteristic Green's function [12]. This type of Green's function expansion was introduced by Schwinger for cylindrical tubes [13, p. 301 and references therein] and waveguide discontinuity problems [14]. The properties of completeness and orthogonality of eigenfunctions in the waveguide cross-section enable the formulation of a Sturm-

Liouville problem for the characteristic Green's function in the waveguiding direction. In fact, it was applied in [15] in the derivation of the magnetic potential Green's dyadic (diagonal tensor) for rectangular waveguides and cavities using scalar eigenfunctions of the Laplacian operator. Important developments of this approach have been reported in the Russian and Ukrainian literature, for example, in [16] for application to three-dimensional waveguide discontinuities and to antenna problems [17], [18]. Electric dyadic Green's functions for a multilayered rectangular waveguide were also developed in [19], [20] with application to shielded printed-circuit transmission lines.

The central contribution of this paper is the presentation of an efficient technique for the rapid development of electric dyadic Green's functions of the third kind of a transversely layered, terminated rectangular waveguide. This technique uses a partial eigenfunction expansion resulting in a Sturm-Liouville problem for one-dimensional characteristic Green's functions in the waveguiding direction. Components of the Green's dyadics are expressed in a double series expansion over the complete system of orthonormal eigenfunctions of the transverse Laplacian operator. The unknown coefficients in this expansion represent one-dimensional characteristic Green's functions along the waveguide. In this representation, transverse and longitudinal coordinates are functionally separated, which allows one to immediately reduce the three-dimensional problem to a one-dimensional Sturm-Liouville boundary value problem for the unknown characteristic Green's functions. The analytical form of obtained characteristic Green's functions provides physical insight into resonance and surface wave effects occurring in overmoded layered waveguide transitions. Specifically, the poles of Green's functions represent the roots of characteristic equations for resonance frequencies of transverse wavenumbers in the layered waveguide cross-section. It occurs that this is associated with the propagation constant (calculated at the resonance frequency) of TE and TM surface waves of the grounded dielectric slab waveguide. At transverse resonance frequency the energy of modes propagating along the waveguide is coupled to the energy of surface waves of the dielectric slab resulting in sharp resonances in the reflection coefficient. This is demonstrated for the examples of 2×3 and 3×4 aperture-coupled patch arrays analyzed in [2], [21].

II. Integral Equation Formulation

Consider the waveguide-based transition module containing arbitrarily shaped interacting electric- (patch, strip) and magnetic-type (slot, aperture) discontinuities as shown in Fig. 1. Regions V_1, V_2, and V_3 are characterized by dielectric materials with permittivities ϵ_1, ϵ_2, and ϵ_3, respectively. The electric-

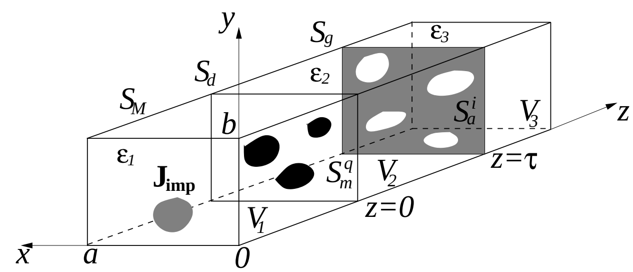

Fig. 1. Waveguide-based transition module of interacting electric- (patch, strip) and magnetic-type (slot, aperture) discontinuities.

type antennas, S_m^q, are located on the transverse interface S_d $(z=0)$ of two adjacent layers with permittivities ϵ_1 and ϵ_2. The magnetic-type antennas, S_a^i, are positioned in the ground plane S_g $(z=\tau)$ which separates regions V_2 and V_3. The problem is formulated for electric currents $\overline{\mathbf{J}}_q(\vec{r}\,')$ and magnetic currents $\overline{\mathbf{M}}_i(\vec{r}\,')$ induced on the surfaces S_m^q and S_a^i, respectively, due to an impressed electric current source $\overline{\mathbf{J}}_{\rm imp}(\vec{r}) \subset V_1$. The integral equation formulation was presented in [1] for a two-port waveguide transition similar to that shown in Fig. 1 (the formulation for an aperture-coupled patch array in an N-port waveguide transition was described in [2]). Here we summarize a system of coupled integral equations obtained for interacting electric- and magnetic-type antennas. The electric-field integral equation is obtained by enforcing a boundary condition for tangential components of the total electric field on metal surfaces S_m^q at $z=0$,

$$\hat{z}\times\overline{\mathbf{E}}_1^{\rm inc}(\vec{r}) = \jmath\omega\mu_0\hat{z}\times\sum_{q=1}^{N}\int_{S_m^q}\overline{\mathbf{J}}_q(\vec{r}\,')\cdot\overline{\overline{\mathbf{G}}}_{e11}^{(1)}(\vec{r}\,',\vec{r})dS' - \hat{z}\times\sum_{i=1}^{M}\int_{S_a^i}\overline{\mathbf{M}}_i(\vec{r}\,')\cdot[\nabla'\times\overline{\overline{\mathbf{G}}}_{e21}^{(1)}(\vec{r}\,',\vec{r})]dS' \quad (1)$$

where $\overline{\mathbf{E}}_1^{\rm inc}$ is the incident electric field due to $\overline{\mathbf{J}}_{\rm imp}$ [1]. The electric Green's dyadics of the third kind, $\overline{\overline{\mathbf{G}}}_{e11}^{(1)}$ and $\overline{\overline{\mathbf{G}}}_{e21}^{(1)}$, are obtained as the solution of the electric-type boundary value problem for a semi-infinite partially filled waveguide (regions V_1 and V_2) terminated by a ground plane at $z=\tau$ (the Green's functions are derived in the section to follow).

The magnetic-field integral equation is obtained by imposing a continuity condition for tangential components of the magnetic field across surfaces S_a^i at $z=\tau$,

$$\hat{z}\times\overline{\mathbf{H}}_2^{\rm inc}(\vec{r}) =$$

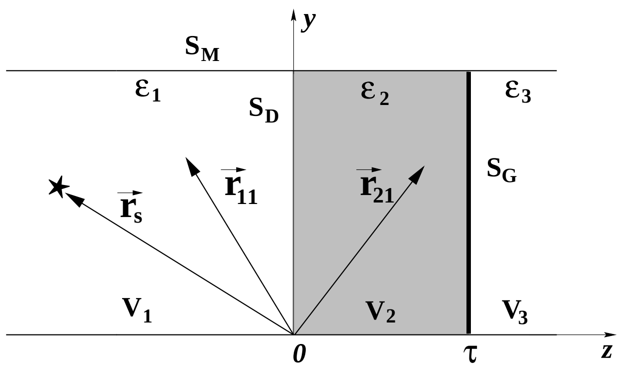

Fig. 2. Two-layered, terminated rectangular waveguide with an electric point source (starred) arbitrarily located in region V_1 used in the electric-field formulation.

$$-\frac{\epsilon_2}{\epsilon_1}\hat{z}\times\sum_{q=1}^{N}\int_{S_m^q}\overline{\mathbf{J}}_q(\vec{r}\,')\cdot[\nabla'\times\overline{\overline{\mathbf{G}}}_{e12}^{(2)}(\vec{r}\,',\vec{r})]dS'$$
$$-\jmath\omega\epsilon_0\hat{z}\times\sum_{i=1}^{M}\int_{S_a^i}\overline{\mathbf{M}}_i(\vec{r}\,')\cdot[\epsilon_2\overline{\overline{\mathbf{G}}}_{e22}^{(2)}(\vec{r}\,',\vec{r})$$
$$+\epsilon_3\overline{\overline{\mathbf{G}}}_{e}^{(2)}(\vec{r}\,',\vec{r})]dS'. \quad (2)$$

Here, $\overline{\mathbf{H}}_2^{\text{inc}}$ is the incident magnetic field at $z=\tau$ due to $\overline{\mathbf{J}}_{\text{imp}}$ in V_1. The electric Green's dyadics of the third kind, $\overline{\overline{\mathbf{G}}}_{e12}^{(2)}$ and $\overline{\overline{\mathbf{G}}}_{e22}^{(2)}$, are obtained as the solution of the magnetic-type boundary value problem for a partially filled, terminated waveguide (the Green's functions are derived in the next section). The electric Green's dyadic of the second kind, $\overline{\overline{\mathbf{G}}}_{e}^{(2)}$, for a semi-infinite rectangular waveguide (region V_3) is described in Appendix of [2]. The coupled system of integral equations (1), (2) is discretized via the Method of Moments resulting in the Generalized Scattering Matrix (GSM) for evanescent and propagating TE and TM modes [1], [2].

III. Electric Green's Dyadics for a Layered Waveguide

A. Electric-Type Boundary-Value Problem

To determine the electric Green's dyadics, a boundary value problem is formulated for a partially filled, terminated rectangular waveguide with a ground plane placed at $z=\tau$ as shown in Fig. 2. The problem is solved in the absence of metal surfaces S_m^q and apertures S_a^i with an electric point source positioned in region V_1. Electric dyadic Green's functions in regions V_1 and V_2 are obtained as the solution of the system of dyadic differential equations [4]:

$$\nabla\times\nabla\times\overline{\overline{\mathbf{G}}}_{e11}^{(1)}(\vec{r},\vec{r}\,')-k_1^2\overline{\overline{\mathbf{G}}}_{e11}^{(1)}(\vec{r},\vec{r}\,')=\overline{\overline{\mathbf{I}}}\delta(\vec{r}-\vec{r}\,'),\quad (3)$$
$$\vec{r},\vec{r}\,'\in V_1$$
$$\nabla\times\nabla\times\overline{\overline{\mathbf{G}}}_{e21}^{(1)}(\vec{r},\vec{r}\,')-k_2^2\overline{\overline{\mathbf{G}}}_{e21}^{(1)}(\vec{r},\vec{r}\,')=0,\quad (4)$$
$$\vec{r}\in V_2\ ,\vec{r}\,'\in V_1$$

subject to boundary conditions of the first kind on the waveguide surface S_M and surface of the ground plane S_G (Fig. 2),

$$\hat{n}\times\overline{\overline{\mathbf{G}}}_{e11}^{(1)}(\vec{r},\vec{r}\,')=0,\qquad \vec{r}\in S_M \quad (5)$$
$$\hat{n}\times\overline{\overline{\mathbf{G}}}_{e21}^{(1)}(\vec{r},\vec{r}\,')=0,\quad \vec{r}\in S_M\cup S_G \quad (6)$$

and mixed continuity conditions for the electric Green's dyadics of the third kind across the dielectric interface S_D:

$$\hat{z}\times\overline{\overline{\mathbf{G}}}_{e11}^{(1)}(\vec{r},\vec{r}\,')=\hat{z}\times\overline{\overline{\mathbf{G}}}_{e21}^{(1)}(\vec{r},\vec{r}\,'),\qquad \vec{r}\in S_D$$
$$\hat{z}\times\nabla\times\overline{\overline{\mathbf{G}}}_{e11}^{(1)}(\vec{r},\vec{r}\,')=\hat{z}\times\nabla\times\overline{\overline{\mathbf{G}}}_{e21}^{(1)}(\vec{r},\vec{r}\,'),\vec{r}\in S_D \quad (7)$$

Here, $k_{1,2}=k_0\sqrt{\epsilon_{1,2}}$, $k_0=2\pi/\lambda_0$; $\hat{n}$ is an outward normal to the surface enclosing volumes V_1 and V_2, respectively. The radiation condition at infinity for the dyadic Green's function $\overline{\overline{\mathbf{G}}}_{e11}^{(1)}$ is also satisfied (similar to the limiting absorption principle for scattered fields [22]).

The solution of the boundary value problem (3)-(7) yields nine components of the electric Green's dyadics, which can be expressed as a partial eigenfunction expansion,

$$\left\{\begin{array}{c}G_{e11}^{(1)\nu\upsilon}\\ G_{e21}^{(1)\nu\upsilon}\end{array}\right\}=$$
$$\sum_{m=0}^{\infty}\sum_{n=0}^{\infty}\phi_{mn}^{(1)\nu}(x,y)\phi_{mn}^{(1)\upsilon}(x',y')\left\{\begin{array}{c}f_{mn}^{(11)\nu\upsilon}(z,z')\\ f_{mn}^{(21)\nu\upsilon}(z,z')\end{array}\right\} \quad (8)$$

for $\nu,\upsilon=x,y,z$, where $\phi_{mn}^{(1)\nu}(x,y)$ are the orthonormal eigenfunctions of the transverse Laplacian operator determined as

$$\phi_{mn}^{(1)x}(x,y)=\sqrt{\frac{\varepsilon_{0m}\varepsilon_{0n}}{ab}}\cos\left(\frac{m\pi x}{a}\right)\sin\left(\frac{n\pi y}{b}\right)$$
$$\phi_{mn}^{(1)y}(x,y)=\sqrt{\frac{\varepsilon_{0m}\varepsilon_{0n}}{ab}}\sin\left(\frac{m\pi x}{a}\right)\cos\left(\frac{n\pi y}{b}\right)$$
$$\phi_{mn}^{(1)z}(x,y)=\sqrt{\frac{\varepsilon_{0m}\varepsilon_{0n}}{ab}}\sin\left(\frac{m\pi x}{a}\right)\sin\left(\frac{n\pi y}{b}\right) \quad (9)$$

and $f_{mn}^{(11)\nu\upsilon}(z,z')$ and $f_{mn}^{(21)\nu\upsilon}(z,z')$ are the one-dimensional characteristic Green's functions. In (9), ε_{0m}, ε_{0n} are Neumann indexes, such that $\varepsilon_{00}=1$ and $\varepsilon_{0m}=2$, $m\neq 0$. Note that the Green's dyadics developed here are used in the integral equation formulations for transverse planar metal conductors and slot apertures. Thus, z-directed current sources are not considered, which eliminates the need to consider Green's function components $G_{e11}^{(1)\nu z}$ and $G_{e21}^{(1)\nu z}$, $\nu = x, y, z$, in the analysis to follow.

Using the properties of orthogonality

$$\int_0^a \int_0^b \phi_{mn}^{(1,2)\nu}(x,y)\phi_{ps}^{(1,2)\nu}(x,y)dydx = \delta_{mp}\delta_{ns} \quad (10)$$

and completeness

$$\sum_{m=0}^{\infty}\sum_{n=0}^{\infty} \phi_{mn}^{(1,2)\nu}(x,y)\phi_{mn}^{(1,2)\nu}(x',y') = \delta(x-x')\delta(y-y') \quad (11)$$

of the eigenfunctions $\phi_{mn}^{(1)\nu}(x,y)$ in the double series expansion (8) allows the system of dyadic differential equations (3) and (4) to be reduced to a system of second-order differential equations for the one-dimensional characteristic Green's functions $f_{mn}^{(11)\nu\upsilon}(z,z')$ and $f_{mn}^{(21)\nu\upsilon}(z,z')$,

$$\left(\frac{\partial^2}{\partial z^2} - \gamma_{mn}^{(1)2}\right) f_{mn}^{(11)\nu\upsilon}(z,z') = -\xi_{mn}^{\nu\upsilon}\delta(z-z') \quad (12)$$
$$\left(\frac{\partial^2}{\partial z^2} - \gamma_{mn}^{(2)2}\right) f_{mn}^{(21)\nu\upsilon}(z,z') = 0, \quad \nu,\upsilon = x,y$$

where

$$\xi_{mn}^{xx} = \frac{k_1^2 - \left(\frac{m\pi}{a}\right)^2}{k_1^2}, \qquad \xi_{mn}^{yy} = \frac{k_1^2 - \left(\frac{n\pi}{b}\right)^2}{k_1^2},$$
$$\xi_{mn}^{xy} = \xi_{mn}^{yx} = -\frac{\left(\frac{m\pi}{a}\right)\left(\frac{n\pi}{b}\right)}{k_1^2}$$

and

$$\gamma_{mn}^{(1,2)} = \sqrt{\left(\frac{m\pi}{a}\right)^2 + \left(\frac{n\pi}{b}\right)^2 - k_{1,2}^2}. \quad (13)$$

The boundary condition (6) on the ground plane S_G, written in terms of the Green's function components, is reduced to the boundary condition for the one-dimensional characteristic Green's functions at $z=\tau$ and $z > z'$,

$$f_{mn}^{(21)\nu\upsilon}(\tau,z') = 0. \quad (14)$$

The continuity conditions (7) on the dielectric interface at $z=0$ and $z>z'$ are obtained as

$$f_{mn}^{(11)\nu\upsilon}(0,z') = f_{mn}^{(21)\nu\upsilon}(0,z'), \quad (15)$$
$$\frac{m\pi}{a} f_{mn}^{(11)z\upsilon}(0,z') - \frac{\partial}{\partial z} f_{mn}^{(11)x\upsilon}(0,z')$$
$$= \frac{m\pi}{a} f_{mn}^{(21)z\upsilon}(0,z') - \frac{\partial}{\partial z} f_{mn}^{(21)x\upsilon}(0,z'), \quad (16)$$
$$\frac{n\pi}{b} f_{mn}^{(11)z\upsilon}(0,z') - \frac{\partial}{\partial z} f_{mn}^{(11)y\upsilon}(0,z')$$
$$= \frac{n\pi}{b} f_{mn}^{(21)z\upsilon}(0,z') - \frac{\partial}{\partial z} f_{mn}^{(21)y\upsilon}(0,z'),$$

and the z-directed Green's functions $f_{mn}^{(11)z\upsilon}$ and $f_{mn}^{(21)z\upsilon}$ introduced in (16) can be expressed in terms of transverse components,

$$f_{mn}^{(i1)z\upsilon} = \frac{1}{\gamma_{mn}^{(i)2}}\frac{\partial}{\partial z}\left(\frac{m\pi}{a} f_{mn}^{(i1)x\upsilon} + \frac{n\pi}{b} f_{mn}^{(i1)y\upsilon}\right) \quad (17)$$

for $i = 1, 2$.

The solution of the system of differential equations (12) is obtained as a superposition of primary and scattered parts,

$$f_{mn}^{(11)\nu\upsilon}(z,z') = \xi_{mn}^{\nu\upsilon}\frac{e^{-\gamma_{mn}^{(1)}|z-z'|}}{2\gamma_{mn}^{(1)}} + \eta_{\nu\upsilon}^{-(11)}(z')e^{\gamma_{mn}^{(1)}z} \quad (18)$$
$$f_{mn}^{(21)\nu\upsilon}(z,z') = \eta_{\nu\upsilon}^{+(21)}(z')e^{-\gamma_{mn}^{(2)}z} + \eta_{\nu\upsilon}^{-(21)}(z')e^{\gamma_{mn}^{(2)}(z-\tau)}. \quad (19)$$

In (18) the primary part is due to a point source positioned in region V_1, and the scattered part represents waves reflected from the interface at $z=0$, traveling in the negative z-direction. In (19) we have only the scattered part which is described by traveling backward and forward waves propagating in region V_2 (between the interface at $z=0$ and the ground plane at $z=\tau$). The unknown η-coefficients to be determined are subject to the boundary and continuity conditions (14) and (15), (16), respectively, and can be obtained in closed form.

Finally, this procedure results in the representation of the one-dimensional transverse characteristic Green's functions $f_{mn}^{(11)\nu\upsilon}(z,z')$ in terms of the primary and scattered parts,

$$f_{mn}^{(11)xx}(z,z') = \xi_{mn}^{xx}\frac{e^{-\gamma_{mn}^{(1)}|z-z'|}}{2\gamma_{mn}^{(1)}} - e^{\gamma_{mn}^{(1)}(z+z')}\left(\frac{\xi_{mn}^{xx}}{2\gamma_{mn}^{(1)}} - \frac{1}{Z_o^{\mathrm{TE}}} + \frac{(\frac{m\pi}{a})^2 Z_e^{\mathrm{TE}}}{k_1^2 Z_o^{\mathrm{TE}} Z_e^{\mathrm{TM}}}\right) \quad (20)$$
$$f_{mn}^{(11)xy}(z,z') = f_{mn}^{(11)yx}(z,z') = \xi_{mn}^{xy} \times\left(\frac{e^{-\gamma_{mn}^{(1)}|z-z'|}}{2\gamma_{mn}^{(1)}} - e^{\gamma_{mn}^{(1)}(z+z')}\left(\frac{1}{2\gamma_{mn}^{(1)}} - \frac{Z_e^{\mathrm{TE}}}{Z_o^{\mathrm{TE}} Z_e^{\mathrm{TM}}}\right)\right)$$
$$f_{mn}^{(11)yy}(z,z') = \xi_{mn}^{yy}\frac{e^{-\gamma_{mn}^{(1)}|z-z'|}}{2\gamma_{mn}^{(1)}} - e^{\gamma_{mn}^{(1)}(z+z')}\left(\frac{\xi_{mn}^{yy}}{2\gamma_{mn}^{(1)}} - \frac{1}{Z_o^{\mathrm{TE}}} + \frac{(\frac{n\pi}{b})^2 Z_e^{\mathrm{TE}}}{k_1^2 Z_o^{\mathrm{TE}} Z_e^{\mathrm{TM}}}\right)$$

and functions $f_{mn}^{(21)\nu\upsilon}(z,z')$ are obtained in terms of scattered waves,

$$f_{mn}^{(21)xx}(z,z') = -\left(\frac{1}{Z_o^{\mathrm{TE}}} - \frac{(\frac{m\pi}{a})^2 Z_e^{\mathrm{TE}}}{k_1^2 Z_o^{\mathrm{TE}} Z_e^{\mathrm{TM}}}\right) \quad (21)$$

$$\times \frac{e^{\gamma_{mn}^{(1)} z'} \sinh \gamma_{mn}^{(2)}(z-\tau)}{\sinh \gamma_{mn}^{(2)} \tau}$$

$$f_{mn}^{(21)xy}(z,z') = f_{mn}^{(21)yx}(z,z') =$$
$$-\xi_{mn}^{xy} \frac{Z_e^{\mathrm{TE}}}{Z_o^{\mathrm{TE}} Z_e^{\mathrm{TM}}} \frac{e^{\gamma_{mn}^{(1)} z'} \sinh \gamma_{mn}^{(2)}(z-\tau)}{\sinh \gamma_{mn}^{(2)} \tau}$$

$$f_{mn}^{(21)yy}(z,z') = -\left(\frac{1}{Z_o^{\mathrm{TE}}} - \frac{(\frac{n\pi}{b})^2 Z_e^{\mathrm{TE}}}{k_1^2 Z_o^{\mathrm{TE}} Z_e^{\mathrm{TM}}}\right)$$
$$\times \frac{e^{\gamma_{mn}^{(1)} z'} \sinh \gamma_{mn}^{(2)}(z-\tau)}{\sinh \gamma_{mn}^{(2)} \tau}.$$

The z-coordinate Green's functions $f_{mn}^{(i1)zx}(z,z')$ and $f_{mn}^{(i1)zy}(z,z')$ for $i = 1, 2$, are determined by (17) with (20) and (21).

Here, $Z_e^{\mathrm{TE}}, Z_o^{\mathrm{TE}}$, and Z_e^{TM} are the characteristic functions of even and odd TE and TM modes, respectively, of a grounded dielectric slab of thickness τ bounded with electric walls at $x = 0, a$ and $y = 0, b$ (region V_2), given as

$$Z_e^{\mathrm{TE}} = \gamma_{mn}^{(1)} + \gamma_{mn}^{(2)} \tanh \gamma_{mn}^{(2)} \tau \qquad (22)$$
$$Z_o^{\mathrm{TE}} = \gamma_{mn}^{(1)} + \gamma_{mn}^{(2)} \coth \gamma_{mn}^{(2)} \tau$$
$$Z_e^{\mathrm{TM}} = \frac{\varepsilon_2}{\varepsilon_1} \gamma_{mn}^{(1)} + \gamma_{mn}^{(2)} \tanh \gamma_{mn}^{(2)} \tau$$

where the propagation constant $\gamma_{mn}^{(1,2)}$ is given by (13) in terms of transverse wave numbers $k_{mn} = \sqrt{(\frac{m\pi}{a})^2 + (\frac{n\pi}{b})^2}$. Zeros of the characteristic functions (22) represent resonance frequencies of TE and TM oscillations in the waveguide cross-section. It can be seen that zeros of Z_o^{TE} and Z_e^{TM} for TE-odd and TM-even modes correspond to poles of the characteristic Green's functions (20) and (21). Moreover, the characteristic functions (22) for an infinite grounded dielectric slab of thickness τ define even and odd TE and TM surface waves with the propagation constant $k_{sw} \equiv k_{mn}$.

At a resonance frequency corresponding to the transverse wavenumber k_{mn} of the shielded grounded dielectric slab, the value of k_{mn} is equal to the value of the propagation constant k_{sw} of a surface wave associated with an infinite dielectric slab. This is related to coupling of waves propagating along the waveguide in the z-direction with propagation constants $\gamma_{mn}^{(1,2)}$ to TE and TM surface waves propagating in an infinite grounded dielectric slab (associated with resonance wavenumbers k_{mn} in the waveguide cross-section). This becomes important in the analysis of waveguide-based aperture-coupled patch amplifier arrays, where coupling to surface waves results in a loss of power and undesirable cross-talk between neighboring antennas.

It should be noted that the characteristic Green's

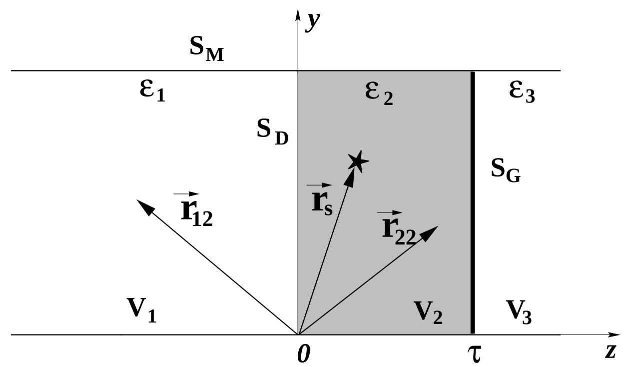

Fig. 3. Two-layered, terminated rectangular waveguide with an electric point source (starred) arbitrarily located in region V_2 used in the magnetic-field formulation.

functions for a transversely layered, terminated waveguide with respect to the wave propagation represent spectral-domain Green's functions for an infinite grounded dielectric slab. The poles of Green's functions in both cases are determined as the zeros of characteristic functions Z_o^{TE} and Z_e^{TM} defined by (22). The difference appears only in the nature of roots of (22). In the closed-boundary layered waveguide they represent resonance frequencies corresponding to discrete transverse wave numbers in the waveguide cross-section. In the case of open-boundary grounded dielectric slab we determine propagation constants of TE and TM surface waves. In this paper we study the correlation between transverse resonances and surface waves by investigating the resonance characteristics of the scattering parameters for the examples of waveguide-based aperture-coupled patch arrays.

B. Magnetic-Type Boundary-Value Problem

The magnetic-type boundary value problem is formulated for the electric Green's dyadics, $\overline{\overline{\mathbf{G}}}_{e12}^{(2)}$ and $\overline{\overline{\mathbf{G}}}_{e22}^{(2)}$, due to an electric point source positioned in region V_2 (Fig. 3). The electric dyadic Green's functions of the third kind are determined as the solution of a coupled set of dyadic differential equations

$$\nabla \times \nabla \times \overline{\overline{\mathbf{G}}}_{e12}^{(2)}(\vec{r}, \vec{r}\,') - k_1^2 \overline{\overline{\mathbf{G}}}_{e12}^{(2)}(\vec{r}, \vec{r}\,') = 0, \qquad (23)$$
$$\vec{r} \in V_1 \,, \vec{r}\,' \in V_2$$

$$\nabla \times \nabla \times \overline{\overline{\mathbf{G}}}_{e22}^{(2)}(\vec{r}, \vec{r}\,') - k_2^2 \overline{\overline{\mathbf{G}}}_{e22}^{(2)}(\vec{r}, \vec{r}\,') = \overline{\overline{\mathbf{I}}}\delta(\vec{r} - \vec{r}\,'), \qquad (24)$$
$$\vec{r}, \vec{r}\,' \in V_2$$

satisfying boundary conditions of the second kind on the surface of a conducting shield S_M and ground plane S_G,

$$\hat{n} \times \nabla \times \overline{\overline{\mathbf{G}}}_{e12}^{(2)}(\vec{r}, \vec{r}\,') = 0 \,, \quad \vec{r} \in S_M \qquad (25)$$

$$\begin{aligned} \hat{n}\cdot\overline{\overline{\mathbf{G}}}^{(2)}_{e12}(\vec{r},\vec{r}\,') = 0\,, \quad & \vec{r}\in S_M \\ \hat{n}\times\nabla\times\overline{\overline{\mathbf{G}}}^{(2)}_{e22}(\vec{r},\vec{r}\,') = 0\,, \quad & \vec{r}\in S_M\cup S_G \\ \hat{n}\cdot\overline{\overline{\mathbf{G}}}^{(2)}_{e22}(\vec{r},\vec{r}\,') = 0\,, \quad & \vec{r}\in S_M\cup S_G \end{aligned} \tag{26}$$

and the mixed continuity conditions for the electric Green's dyadics of the third kind across the dielectric interface S_D,

$$\begin{aligned} \hat{z}\times\overline{\overline{\mathbf{G}}}^{(2)}_{e12}(\vec{r},\vec{r}\,') &= \hat{z}\times\overline{\overline{\mathbf{G}}}^{(2)}_{e22}(\vec{r},\vec{r}\,'), \\ & \qquad \vec{r}\in S_D \\ \frac{1}{\epsilon_1}\hat{z}\times\nabla\times\overline{\overline{\mathbf{G}}}^{(2)}_{e12}(\vec{r},\vec{r}\,') &= \frac{1}{\epsilon_2}\hat{z}\times\nabla\times\overline{\overline{\mathbf{G}}}^{(2)}_{e22}(\vec{r},\vec{r}\,'), \\ & \qquad \vec{r}\in S_D. \end{aligned} \tag{27}$$

Note that the radiation condition at infinity for the Green's function $\overline{\overline{\mathbf{G}}}^{(2)}_{e12}$ is also satisfied.

The solution of the boundary value problem (23)-(27) can be expressed in the form of a partial eigenfunction expansion,

$$\left\{\begin{array}{c} G^{(2)\nu\upsilon}_{e12} \\ G^{(2)\nu\upsilon}_{e22} \end{array}\right\} = \sum_{m=0}^{\infty}\sum_{n=0}^{\infty}\phi^{(2)\nu}_{mn}(x,y)\phi^{(2)\upsilon}_{mn}(x',y')\left\{\begin{array}{c} g^{(12)\nu\upsilon}_{mn}(z,z') \\ g^{(22)\nu\upsilon}_{mn}(z,z') \end{array}\right\} \tag{28}$$

for $\nu,\upsilon = x,y,z$, where $\phi^{(2)\nu}_{mn}(x,y)$ are the second-kind orthonormal eigenfunctions of the transverse Laplacian operator given by

$$\begin{aligned} \phi^{(2)x}_{mn}(x,y) &= \sqrt{\frac{\varepsilon_{0m}\varepsilon_{0n}}{ab}}\sin\left(\frac{m\pi x}{a}\right)\cos\left(\frac{n\pi y}{b}\right) \\ \phi^{(2)y}_{mn}(x,y) &= \sqrt{\frac{\varepsilon_{0m}\varepsilon_{0n}}{ab}}\cos\left(\frac{m\pi x}{a}\right)\sin\left(\frac{n\pi y}{b}\right) \\ \phi^{(2)z}_{mn}(x,y) &= \sqrt{\frac{\varepsilon_{0m}\varepsilon_{0n}}{ab}}\cos\left(\frac{m\pi x}{a}\right)\cos\left(\frac{n\pi y}{b}\right) \end{aligned} \tag{29}$$

and $g^{(12)\nu\upsilon}_{mn}(z,z')$ and $g^{(22)\nu\upsilon}_{mn}(z,z')$ are the one-dimensional characteristic Green's functions to be determined as the solution of a Sturm-Liouville problem. As in the case of the electric-type boundary value problem discussed above, the longitudinal components $G^{(2)\nu z}_{e12}$ and $G^{(2)\nu z}_{e22}$ for $\nu = x,y,z$ do not appear in the formulation for the magnetic field (2) and will not be considered here.

A system of second-order differential equations for the one-dimensional characteristic Green's functions $g^{(12)\nu\upsilon}_{mn}(z,z')$ and $g^{(22)\nu\upsilon}_{mn}(z,z')$ is obtained from (23) and (24) using properties of orthogonality (10) and completeness (11) of the eigenfunctions $\phi^{(2)\nu}_{mn}(x,y)$,

$$\left(\frac{\partial^2}{\partial z^2} - \gamma^{(1)2}_{mn}\right) g^{(12)\nu\upsilon}_{mn}(z,z') = 0, \quad \nu,\upsilon = x,y \tag{30}$$

$$\left(\frac{\partial^2}{\partial z^2} - \gamma^{(2)2}_{mn}\right) g^{(22)\nu\upsilon}_{mn}(z,z') = -\zeta^{\nu\upsilon}_{mn}\delta(z-z')$$

where

$$\zeta^{xx}_{mn} = \frac{k_2^2 - \left(\frac{m\pi}{a}\right)^2}{k_2^2}, \qquad \zeta^{yy}_{mn} = \frac{k_2^2 - \left(\frac{n\pi}{b}\right)^2}{k_2^2},$$

$$\zeta^{xy}_{mn} = \zeta^{yx}_{mn} = -\frac{\left(\frac{m\pi}{a}\right)\left(\frac{n\pi}{b}\right)}{k_2^2}.$$

The boundary conditions for the transverse characteristic Green's functions at $z=\tau$ and $z>z'$ are obtained directly from (26) using the eigenfunction expansion (28),

$$\frac{\partial}{\partial z} g^{(22)\nu\upsilon}_{mn}(\tau,z') = 0 \tag{31}$$

and the continuity conditions (27) are reduced to the continuity conditions for the one-dimensional Green's functions determined on the dielectric interface at $z=0$ and $z<z'$,

$$g^{(12)\nu\upsilon}_{mn}(0,z') = g^{(22)\nu\upsilon}_{mn}(0,z'), \tag{32}$$

$$\begin{aligned} &\frac{1}{\varepsilon_1}\left(\frac{m\pi}{a}g^{(12)z\upsilon}_{mn}(0,z') + \frac{\partial}{\partial z}g^{(12)x\upsilon}_{mn}(0,z')\right) \\ &= \frac{1}{\varepsilon_2}\left(\frac{m\pi}{a}g^{(22)z\upsilon}_{mn}(0,z') + \frac{\partial}{\partial z}g^{(22)x\upsilon}_{mn}(0,z')\right), \\ &\frac{1}{\varepsilon_1}\left(\frac{n\pi}{b}g^{(12)z\upsilon}_{mn}(0,z') + \frac{\partial}{\partial z}g^{(12)y\upsilon}_{mn}(0,z')\right) \\ &= \frac{1}{\varepsilon_2}\left(\frac{n\pi}{b}g^{(22)z\upsilon}_{mn}(0,z') + \frac{\partial}{\partial z}g^{(22)y\upsilon}_{mn}(0,z')\right). \end{aligned} \tag{33}$$

The z-directed characteristic Green's functions $g^{(12)z\upsilon}_{mn}$ and $g^{(22)z\upsilon}_{mn}$ introduced in (33) are obtained in terms of transverse Green's functions as

$$g^{(i2)z\upsilon}_{mn} = -\frac{1}{\gamma^{(i)2}_{mn}}\frac{\partial}{\partial z}\left(\frac{m\pi}{a}g^{(i2)x\upsilon}_{mn} + \frac{n\pi}{b}g^{(i2)y\upsilon}_{mn}\right) \tag{34}$$

for $i=1,2$.

The solution of the system of second-order differential equations (30) is given by a superposition of primary and scattered parts,

$$g^{(12)\nu\upsilon}_{mn}(z,z') = \theta^{-(12)}_{\nu\upsilon}(z')e^{\gamma^{(1)}_{mn}z} \tag{35}$$

$$\begin{aligned} g^{(22)\nu\upsilon}_{mn}(z,z') &= \zeta^{\nu\upsilon}_{mn}\frac{e^{-\gamma^{(2)}_{mn}|z-z'|}}{2\gamma^{(2)}_{mn}} \\ &\quad + \theta^{+(22)}_{\nu\upsilon}(z')e^{-\gamma^{(2)}_{mn}z} + \theta^{-(22)}_{\nu\upsilon}(z')e^{\gamma^{(2)}_{mn}(z-\tau)}. \end{aligned} \tag{36}$$

In (35) we have only backward traveling waves propagating in the negative z-direction in region V_1. In (36) the solution is represented by the primary Green's function due to a point source positioned in region V_2, and the scattered part is a superposition of backward and forward traveling waves propagating in region V_2 (between the interface at $z = 0$ and the ground plane at $z = \tau$). The unknown θ-coefficients are determined subject to the boundary and continuity conditions (31) and (32), (33), respectively.

The one-dimensional transverse characteristic Green's functions $g_{mn}^{(12)\nu\upsilon}(z,z')$ are obtained as

$$g_{mn}^{(12)xx}(z,z') = \left(\frac{1}{Z_e^{\mathrm{TM}}} - \frac{(\frac{m\pi}{a})^2 Z}{k_2^2 Z_o^{\mathrm{TE}} Z_e^{\mathrm{TM}}}\right) \times \frac{e^{\gamma_{mn}^{(1)} z}\cosh\gamma_{mn}^{(2)}(z'-\tau)}{\cosh\gamma_{mn}^{(2)}\tau} \tag{37}$$

$$g_{mn}^{(12)xy}(z,z') = g_{mn}^{(12)yx}(z,z') = \zeta_{mn}^{xy}\frac{Z}{Z_o^{\mathrm{TE}}Z_e^{\mathrm{TM}}}\frac{e^{\gamma_{mn}^{(1)} z}\cosh\gamma_{mn}^{(2)}(z'-\tau)}{\cosh\gamma_{mn}^{(2)}\tau}$$

$$g_{mn}^{(12)yy}(z,z') = \left(\frac{1}{Z_e^{\mathrm{TM}}} - \frac{(\frac{n\pi}{b})^2 Z}{k_2^2 Z_o^{\mathrm{TE}} Z_e^{\mathrm{TM}}}\right) \times \frac{e^{\gamma_{mn}^{(1)} z}\cosh\gamma_{mn}^{(2)}(z'-\tau)}{\cosh\gamma_{mn}^{(2)}\tau}$$

and transverse Green's functions $g_{mn}^{(22)\nu\upsilon}(z,z')$ are determined in terms of the primary and scattered parts,

$$g_{mn}^{(22)xx}(z,z') = \zeta_{mn}^{xx}\frac{e^{-\gamma_{mn}^{(2)}|z-z'|}}{2\gamma_{mn}^{(2)}} + \zeta_{mn}^{xx}\frac{e^{\gamma_{mn}^{(2)}(z+z'-2\tau)}}{2\gamma_{mn}^{(2)}} + \left(\frac{k_2^2 Z_o^{\mathrm{TE}} - (\frac{m\pi}{a})^2 Z}{k_2^2 Z_o^{\mathrm{TE}} Z_e^{\mathrm{TM}}\cosh\gamma_{mn}^{(2)}\tau} - \frac{\zeta_{mn}^{xx} e^{-\gamma_{mn}^{(2)}\tau}}{\gamma_{mn}^{(2)}}\right) \times \frac{\cosh\gamma_{mn}^{(2)}(z-\tau)\cosh\gamma_{mn}^{(2)}(z'-\tau)}{\cosh\gamma_{mn}^{(2)}\tau} \tag{38}$$

$$g_{mn}^{(22)xy}(z,z') = g_{mn}^{(22)yx}(z,z') = \zeta_{mn}^{xy}\frac{e^{-\gamma_{mn}^{(2)}|z-z'|}}{2\gamma_{mn}^{(2)}} + \zeta_{mn}^{xy}\frac{e^{\gamma_{mn}^{(2)}(z+z'-2\tau)}}{2\gamma_{mn}^{(2)}} + \zeta_{mn}^{xy}\left(\frac{Z}{Z_o^{\mathrm{TE}} Z_e^{\mathrm{TM}}\cosh\gamma_{mn}^{(2)}\tau} - \frac{e^{-\gamma_{mn}^{(2)}\tau}}{\gamma_{mn}^{(2)}}\right) \times \frac{\cosh\gamma_{mn}^{(2)}(z-\tau)\cosh\gamma_{mn}^{(2)}(z'-\tau)}{\cosh\gamma_{mn}^{(2)}\tau}$$

$$g_{mn}^{(22)yy}(z,z') = \zeta_{mn}^{yy}\frac{e^{-\gamma_{mn}^{(2)}|z-z'|}}{2\gamma_{mn}^{(2)}} + \zeta_{mn}^{yy}\frac{e^{\gamma_{mn}^{(2)}(z+z'-2\tau)}}{2\gamma_{mn}^{(2)}} + \left(\frac{k_2^2 Z_o^{\mathrm{TE}} - (\frac{n\pi}{b})^2 Z}{k_2^2 Z_o^{\mathrm{TE}} Z_e^{\mathrm{TM}}\cosh\gamma_{mn}^{(2)}\tau} - \frac{\zeta_{mn}^{yy} e^{-\gamma_{mn}^{(2)}\tau}}{\gamma_{mn}^{(2)}}\right) \times \frac{\cosh\gamma_{mn}^{(2)}(z-\tau)\cosh\gamma_{mn}^{(2)}(z'-\tau)}{\cosh\gamma_{mn}^{(2)}\tau}$$

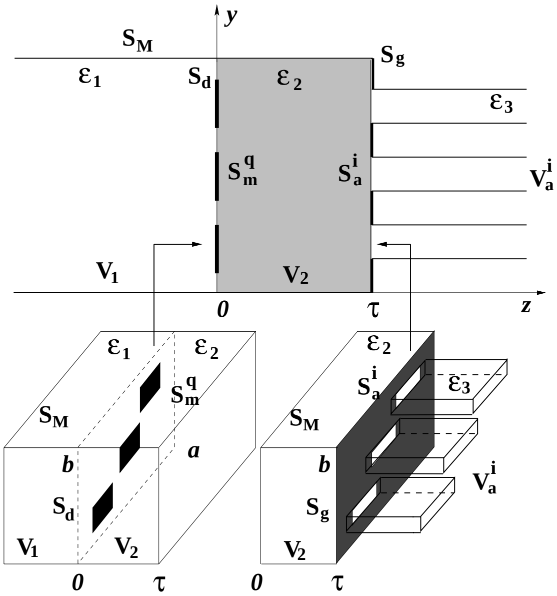

Fig. 4. A waveguide-based aperture-coupled patch array in the N-port waveguide transition.

where $Z = \gamma_{mn}^{(1)} + \frac{\varepsilon_2}{\varepsilon_1}\gamma_{mn}^{(2)}\coth\gamma_{mn}^{(2)}\tau$. Poles of the Green's functions $g_{mn}^{(12)\nu\upsilon}(z,z')$ and $g_{mn}^{(22)\nu\upsilon}(z,z')$ represent zeros of characteristic functions corresponding to the resonance frequencies of TE-odd and TM-even oscillations in the layered waveguide cross-section.

The z-directed Green's functions $g_{mn}^{(i2)zx}(z,z')$ and $g_{mn}^{(i2)zy}(z,z')$, $i = 1,2$, can be obtained from (34) using the expressions for the transverse Green's functions (37) and (38).

IV. Numerical Results and Discussion

The integral equation formulation and the electric dyadic Green's functions presented in this paper were implemented in the numerical algorithm for the GSM of an aperture-coupled patch array in the N-port waveguide transition (Fig. 4). The GSM parameters generated were used in the cascading scheme to determine an overall response (return loss and gain) of a waveguide-based aperture-coupled patch amplifier array [2].

The accuracy of the full-wave modeling has been verified by performing an experiment for a single unit cell (Fig. 5) at X-band (see also [2]). The unit cell contains an aperture-coupled patch antenna and a waveguide-to-microstrip transition. The latter transition was used in the active patch array to feed am-

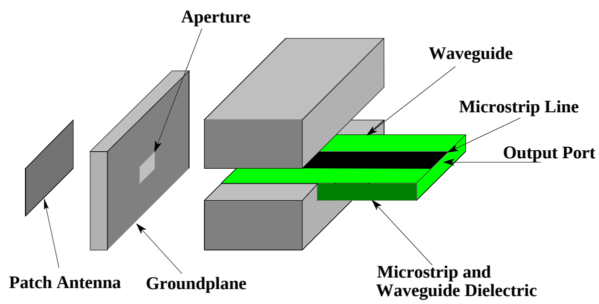

Fig. 5. A rectangular patch antenna coupled through slot to a waveguide-to-microstrip line junction.

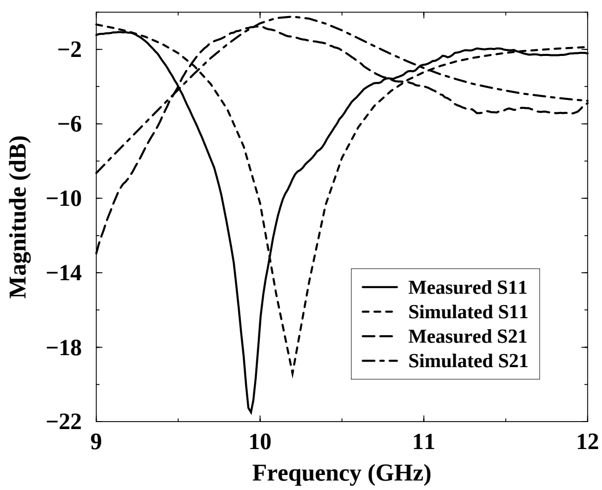

Fig. 6. Numerical and experimental results for the reflection and transmission coefficient of the single unit cell, including a waveguide-based aperture-coupled patch antenna and a waveguide-to-microstrip line junction.

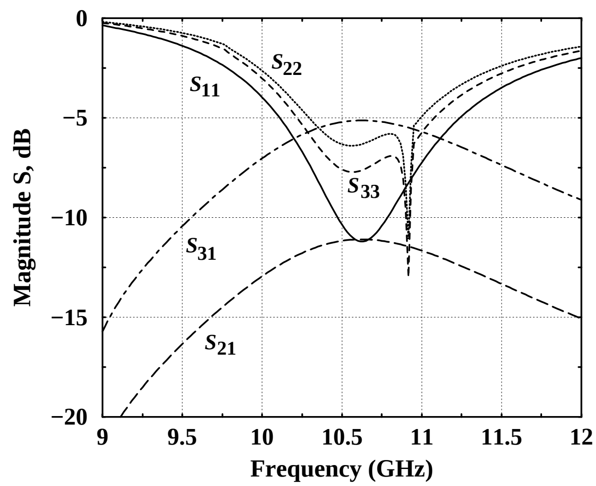

Fig. 7. Magnitude of the S-parameters versus frequency for the 2×3 aperture-coupled patch array in the 7-port rectangular waveguide transition.

plifiers (modeling and experiments for the amplifier array are discussed in [2], [21], [23]). In the measurement of a passive structure, a WR90 waveguide and coaxial transmission line were used to feed the patch antenna and microstrip line, respectively. The patch antenna has 340 mil (8.636 mm) width and 320 mil (8.128 mm) height, slot is of 250 mil (6.35 mm) width and 15 mil (0.381 mm) height, and substrate thickness is 31 mil (0.7874 mm) with permittivity of 2.2. The dielectric-filled waveguide has 450 mil (11.43 mm) width, 15 mil (0.381 mm) height, and 100 mil (2.54 mm) length. The length of the microstrip line is 1800 mil (45.72 mm), and the width is 45 mil (1.143 mm). The numerical results for the scattering parameters of the waveguide-to-microstrip line junction were generated using *Agilent HFSS* and cascaded with the full-wave results (scattering parameters) of a waveguide-based aperture-coupled patch antenna generated by the integral equation method described here and in [1], [2]. The frequency-dependent characteristics of the reflection and transmission coefficient of the complete unit cell (a waveguide-based aperture-coupled patch antenna and a waveguide-to-microstrip line junction) are shown in Fig. 6. The reference plane for the reflection coefficient S_{11} is at $z = 0$ (position of the patch antenna with respect to the excitation) and the reference plane for the transmission coefficient S_{21} is at the end of the microstrip line (see "Output Port" in Fig. 5). The dispersion behavior and the resonance frequency simulated are compared well with the experimental data.

Numerical results for the S-parameters (magnitude and phase) of the dominant TE_{10} mode in the 2×3 aperture-coupled patch array waveguide transition operating at X-band (similar to the N-port waveguide transition shown in Fig. 4) are shown in Figs. 7 and 8 . The geometrical and material parameters for patch and slot antennas are the same as in the example of a single unit cell. The large waveguide (regions V_1 and V_2 in Fig. 4) has 1200.787 mil (30.5 mm) height and 1811.024 mil (46. mm) width, and the small waveguides (regions V_a^i in Fig. 4) have 450 mil (11.43 mm) width and 15 mil (0.381 mm) height. Unit cells in the array are separated by a distance of 600 mil (15.24 mm). In Figs. 7 and 8, S_{11} is the reflection coefficient at the interface $z = 0$ in region V_1 (with the excitation from V_1), and S_{22} and S_{33} are the reflection coefficients at $z = \tau$ (ground plane) in regions V_a^2 and V_a^3 (with the excitation from V_a^2 and V_a^3, respectively). Note that other waveguides V_a^i in the 2×3 array are symmetric to V_a^2 and V_a^3. The port numbering in the array starts with the lower row of

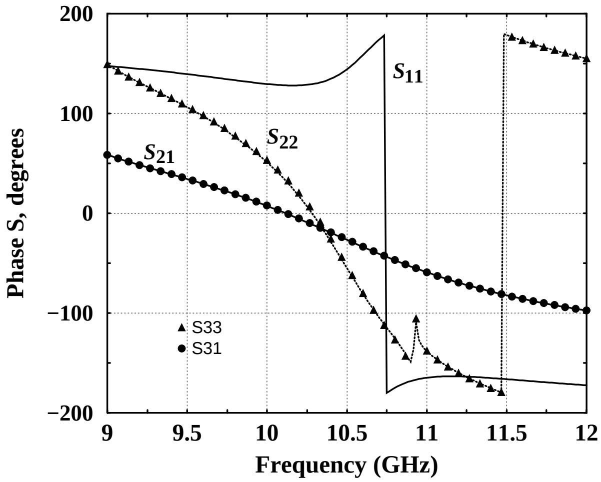

Fig. 8. Phase of the S-parameters versus frequency for the 2×3 aperture-coupled patch array in the 7-port rectangular waveguide transition.

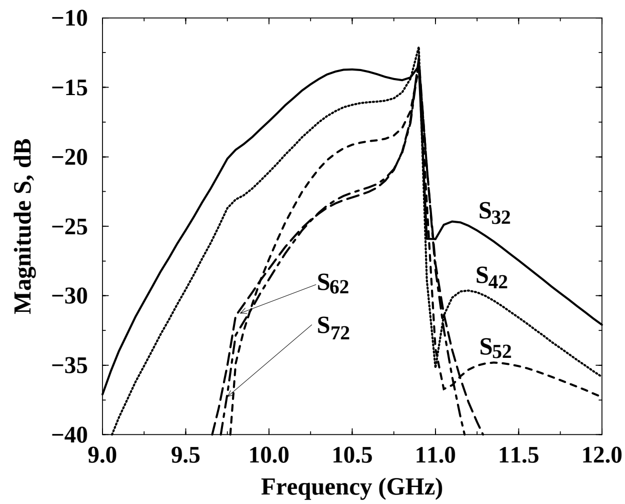

Fig. 10. Port-to-port coupling in the 2×3 aperture-coupled patch array.

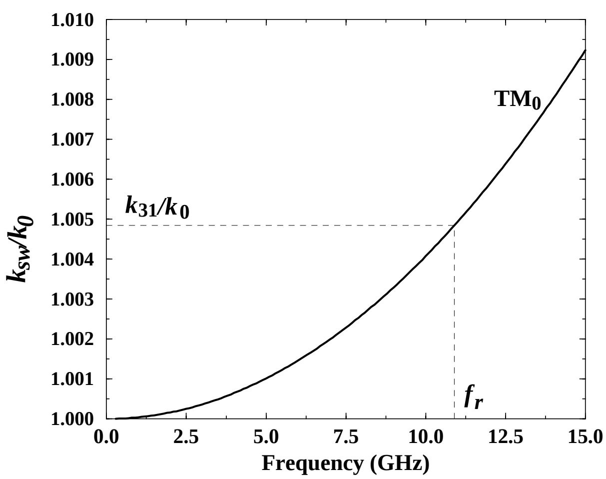

Fig. 9. Dispersion behavior of the normalized propagation constant of the dominant TM_0 mode in a grounded dielectric slab waveguide.

antenna elements (port number 2, 3, and 4) and continues to the upper row (port number 5, 6, and 7). The transmission coefficients from V_1 into V_a^2 and V_a^3 are denoted as S_{21} and S_{31}, respectively. The sharp resonance obtained at f_r=10.8965 GHz corresponds to the occurrence of a transverse resonance, and is associated with the coupling of a mode propagating along the waveguide to the surface wave TM_0 of a dielectric slab (substrate) propagating in the transverse direction (waveguide cross-section).

The dispersion behavior of the normalized propagation constant k_{sw}/k_0 of the dominant TM_0 mode in a grounded dielectric slab waveguide is shown in Fig. 9. The transverse wave number k_{mn} at the resonance frequency f_r corresponds to k_{31} ($m=3$, $n=1$) and its normalized value $k_{31}/k_0 = k_{sw}/k_0$ is equal to 1.00484. This phenomenon is discussed in the previous section in the analysis of Green's function components. Note that for the geometrical and material parameters of the substrate considered in this example, only TM_0 proper mode will propagate (other proper TM-even and TE-odd modes are cutoff at X-band). In the example of a single unit cell considered above in the X-band waveguide there are no discrete wave numbers k_{mn} which are resonant in the layered waveguide cross-section in the frequency range from 9 GHz to 12 GHz (no zeros of the characteristic functions Z_o^{TE} and Z_e^{TM}, even though the surface wave TM_0 of the dielectric slab propagates at all the frequencies).

Port-to-port coupling is studied for the example of a 2×3 aperture-coupled patch array in the 7-port rectangular waveguide transition (Fig. 10). The excitation is considered at port 2 (region V_a^2) with the reference plane at $z=\tau$. The transmission coefficients S_{i2}, $i=3,...,7$ correspond to the coupling of energy from the waveguide V_a^2 to the waveguides V_a^i through the slot apertures at $z=\tau$ (reference plane for transmission). It can be seen that at the resonance frequency, associated with the coupling to the surface wave of the dielectric slab, the port-to-port transmission characteristics are significantly perturbed. Fig. 10 shows the resonance nature of the S-parameters at f_r=10.8965 GHz.

Numerical results were also obtained for a 3×4 waveguide-based aperture-coupled patch array (13-port waveguide transition). The large waveguide in the transition has 2125 mil (53.975 mm) height and

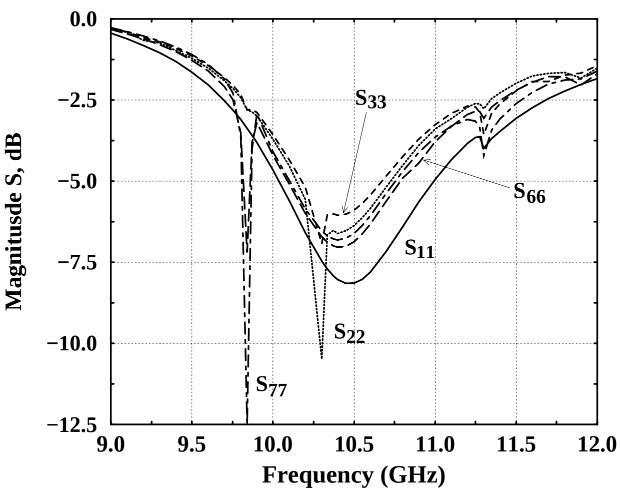

Fig. 11. Magnitude of the reflection coefficients versus frequency for the 3×4 aperture-coupled patch array in the 13-port rectangular waveguide transition.

2875 mil (73.025 mm) width. Magnitude of the reflection coefficients with the excitation at ports 1, 2, 3, 6, and 7 (regions V_1, V_a^2, V_a^3, V_a^6, and V_a^7), respectively, is shown in Fig. 11. Note that other ports in the transition are symmetric to ports 2, 3, 6, and 7. The nature of the sharp resonances observed for the reflection coefficients in Fig. 11 can also be explained by the occurrence of transverse resonances in the waveguide cross-section. It can be seen that an increase of the waveguide size results in an increase in the number of transverse resonances corresponding to coupling of waveguide modes to the surface wave TM_0. Also note that the propagation constants $\gamma_{mn}^{(1,2)}$ (modes propagating in regions V_1 and V_2 in the waveguiding direction), which are associated with transverse resonances for certain m and n, behave in such a way that $\gamma_{mn}^{(1)}$ represent an evanescent mode in region V_1 and $\gamma_{mn}^{(2)}$ correspond to propagating mode in region V_2 at the transverse resonance frequency. This is similar to dispersion characteristics of surface waves propagating in a grounded dielectric slab.

V. Conclusion

In this paper, an efficient technique for developing electric dyadic Green's functions with an electric point source was presented for a partially filled, terminated rectangular waveguide. These Green's functions are used in the integral equation formulation for the full-wave analysis of waveguide-based aperture-coupled patch arrays. The electric-type and magnetic-type boundary value problems are formulated for electric Green's dyadics of the third kind. The components of Green's functions are expressed as a partial eigenfunction expansion. This representation, wherein transverse and longitudinal coordinates are functionally separated, enables the initial dyadic problem to be immediately reduced to the Sturm-Liouville problem for one-dimensional characteristic Green's functions using properties of completeness and orthogonality of transverse eigenfunctions. The characteristic Green's functions are obtained by a superposition of primary and scattered parts subject to boundary and continuity conditions. The analytical form of the obtained characteristic Green's functions provides physical insight into resonance and surface wave effects occurring in overmoded layered waveguide transitions. This was demonstrated for the examples of aperture-coupled patch arrays in the N-port waveguide transition, although the analysis is applicable to other waveguide-based antenna structures, which allow for the propagation of surface waves.

VI. Acknowledgments

This work was supported by an Army Research Office MURI grant, under the Spatial and Quasi-Optical Power Combining DAAG-55-97-0132. Sean Ortiz was also supported by a NSF Graduate Fellowship. The authors would like to thank Prof. George W. Hanson from the University of Wisconsin-Milwaukee, USA, for helpful discussions and comments.

References

[1] A. B. Yakovlev, A. I. Khalil, C. W. Hicks, A. Mortazawi, and M. B. Steer, "The generalized scattering matrix of closely spaced strip and slot layers in waveguide," *IEEE Trans. Microwave Theory Tech.*, Vol. 48, pp. 126–137, Jan. 2000.

[2] A. B. Yakovlev, S. Ortiz, M. Ozkar, A. Mortazawi, and M. B. Steer, "A Waveguide-based aperture-coupled patch amplifier array — Full-wave system analysis and experimental validation," *IEEE Trans. Microwave Theory Tech.*, Vol. 48, pp. 2692–2699, Dec. 2000.

[3] P. M. Morse and H. Feshbach, *Methods of Theoretical Physics.* McGraw-Hill, New York, 1953.

[4] C.-T. Tai, *Dyadic Green Functions in Electromagnetic Theory.* IEEE Press, New Jersey, 1993.

[5] R. E. Collin, *Field Theory of Guided Waves.* IEEE Press, New Jersey, 1991.

[6] L. W. Li, P.-S. Kooi, M.-S. Leong, T.-S. Yeo, and S.-L. Ho, "On the eigenfunction expansion of electromagnetic dyadic Green's functions in rectangular cavities and waveguides," *IEEE Trans. Microwave Theory Tech.*, Vol. 43, No. 3, pp. 700–702, 1995.

[7] C.-T. Tai and P. Rozenfeld, "Different representations of dyadic Green's functions for a rectangular cavity," *IEEE Trans. Microwave Theory Tech.*, Vol. 24, No. 9, pp. 597–601, 1976.

[8] P. H. Pathak, "On the eigenfunction expansion of electromagnetic dyadic Green's functions," *IEEE Trans. Antennas Propagation*, Vol. 31, No. 6, pp. 837–846, Nov. 1983.

[9] L. W. Li, P.-S. Kooi, M.-S. Leong, and T.-S. Yeo, "Full-wave analysis of antenna radiation in a rectangular waveguide with discontinuity: Part I – Dyadic Green's function," *Proc. of ICCS Conf.*, Singapore, Vol. 2, pp. 459–463, 1994.

[10] H. Jin, W. Lin, and Y. Lin, "Dyadic Green's functions for rectangular waveguide filled with longitudinally multilayered isotropic dielectric and their application," *IEE Proc.-Microwave Antennas Propagat.*, Vol. 141, No. 6, pp. 504–508, 1994.

[11] L. W. Li, P.-S. Kooi, M.-S. Leong, T.-S. Yeo, and S.-L. Ho, "Input impedance of a probe-excited semi-infinite rectangular waveguide with arbitrary multilayered loads: Part I – Dyadic Green's functions," *IEEE Trans. Microwave Theory Tech.*, Vol. 43, No. 7, pp. 1559–1566, 1995.

[12] L. B. Felsen and N. Marcuvitz, *Radiation and Scattering of Waves.* IEEE Press, New Jersey, 1994.

[13] F. E. Borgnis and C. H. Papas, *Electromagnetic Waveguides and Resonators. Handbuch Der Physik, XVI.* Springer-Verlag, Berlin, 1958.

[14] J. Schwinger and D. S. Saxon, *Discontinuities in Waveguides.* Gordon and Breach Science Publishers, New York, 1968.

[15] Y. Rahmat-Samii, "On the question of computation of the dyadic Green's function at the source region in waveguides and cavities," *IEEE Trans. Microwave Theory Tech.*, Vol. 23, No. 9, pp. 762–765, 1975.

[16] I. G. Prokhoda, S. G. Dmitryuk, and V. M. Morozov, Tensor Green's Functions with Applications in Microwave Electrodynamics. Dniepropetrovsk: Dniepropetrovsk State University, Ukraine, 1985 (In Russian).

[17] S. G. Dmitryuk and I. V. Petrusenko, "The numerical analytical method of solving three-dimensional diffraction problems in the complex geometry domain," *Mathematical Methods in EM Theory Int. Conf.*, Kharkov, Ukraine, pp. 75–78, 1994.

[18] I. V. Petrusenko and S. G. Dmitryuk, "The method of partial overlapping regions for analysis the waveguide discontinuity and antenna problems," *URSI EM Theory Int. Symp.*, St.-Petersburg, Russia, pp. 52–54, 1995.

[19] A. B. Gnilenko, A. B. Yakovlev, and I. V. Petrusenko, "Generalised approach to modelling shielded printed-circuit transmission lines," *IEE Proc.-Microwave Antennas Propagat.*, Vol. 144, No. 2, pp. 103–110, 1997.

[20] A. B. Gnilenko and A. B. Yakovlev, "Electric dyadic Green functions for applications to shielded multilayered transmission line problems," *IEE Proc.-Microwave Antennas Propagat.*, Vol. 146, No. 2, pp. 111–118, 1999.

[21] A. B. Yakovlev, S. Ortiz, M. Ozkar, A. Mortazawi, and M. B. Steer, "Electromagnetic modeling and experimental verification of a complete waveguide-based aperture-coupled patch amplifier array," *IEEE Int. Microwave Symp. Dig.*, pp. 801–804, June 2000.

[22] A. I. Nosich, "Radiation conditions, limiting absorption principle, and general relations in open waveguide scattering," *J. Electromagn. Waves Applications*, Vol. 8, No. 3, pp. 329–353, 1994.

[23] S. Ortiz, M. Ozkar, A.B. Yakovlev, M.B. Steer, and A. Mortazawi, "Fault tolerance analysis and measurement of a spatial power amplifier," *IEEE Int. Microwave Symp. Dig.*, pp. 1827–1830, May 2001.

Alexander B. Yakovlev received the Ph.D. degree in Radiophysics from the Institute of Radiophysics and Electronics, National Academy of Sciences, Ukraine, in 1992, and the Ph.D. degree in Electrical Engineering from the University of Wisconsin at Milwaukee, in 1997. In summer of 2000, he joined the Department of Electrical Engineering, The University of Mississippi, University, as an Assistant Professor. His research interests include mathematical methods in applied electromagnetics, modeling of high-frequency interconnection structures and amplifier arrays for spatial and quasi-optical power combining, integrated-circuit elements and devices, theory of leaky waves, and singularity theory.

Dr. Yakovlev received the Young Scientist Award presented at the 1992 URSI International Symposium on Electromagnetic Theory, Sydney, Australia, and the Young Scientist Award at the 1996 International Symposium on Antennas and Propagation, Chiba, Japan. He is a member of URSI Commission B.

Sean Ortiz received the B.S.E.E. and M.S.E.E. degrees from the University of Central Florida, Orlando, in 1996 and 1998, respectively, and the Ph.D. degree in electrical engineering from North Carolina State University, Raleigh, in 2001. His research interests include quasi-optical power-combining amplifiers, electromagnetically hardened horns, and transmit-receive antennas.

Dr. Ortiz is a National Science Foundation Graduate Fellow and a member of Tau Beta Pi.

Mete Ozkar received the B.S. degree in Electrical Engineering at the Middle East Technical University, his M.S. and Ph.D degrees in Electrical Engineering at North Carolina State University in 1998 and 2001, respectively. While pursuing the B.S. degree he worked as a co-op for Aerodata, Braunschweig Germany in the summer of 1995. He has been holding a Research Assistantship with the Electronics Research Laboratory in the Department of Electrical and Computer Engineering since 1996. His research interests include analog and RF circuit design, microwave systems, electromagnetic and circuit analysis of spatial power combining systems, and computer aided simulation of nonlinear circuits. He is a member of the Institute of Electrical and Electronic Engineers and the Microwave Theory and Techniques Society since 1997.

Amir Mortazawi received the B.S. degree in electrical engineering from the State University of New York at Stony Brook, in 1987, and the M.S. and Ph.D. degrees in electrical engineering from the University of Texas at Austin, in 1988 and 1990, respectively. In 1990, he joined the University of Central Florida, Orlando, as an Assistant Professor, and became an Associate Professor in 1995. In August of 1998, he joined the North Carolina State University, Raleigh, as an Associate Professor of electrical engineering. In August 2001, he joined the Department of Electrical Engineering and Computer Science, The University of Michigan at Ann Arbor, where he is currently an Associate Professor of electrical engineering. His research interests include millimeter-wave power-combining oscillators and amplifiers, QO techniques, and frequency agile microwave circuits.

Dr. Mortazawi was an associate editor for the IEEE Transactions on Antennas and Propagation.

Michael B. Steer received his B.E. and Ph.D. in Electrical Engineering from the University of Queensland, Brisbane, Australia, in 1978 and 1983 respectively. Currently he is Professor in the Department of Electrical and Computer Engineering at North Carolina State University. His research work has been closely tied to solving fundamental problems in modeling and implementing high-speed digital and microwave circuits. Currently his interests in RF and microwave design are in linearization of efficient power amplifiers, spatial power combining systems; design of millimeter-wave and terahertz frequency electronic circuits, high efficiency low cost RF technologies for wireless applications; and computer-aided engineering of mixed digital, analog and microwave circuits. More generally his work is directed at global modeling of microwave and millimeter-wave systems incorporating fields, circuits, devices, thermal and mechanical effects so that entire electronic systems can be modeled. He is working on developing a new paradigm for the design of spatially distributed millimeter-wave systems.

Professor Steer is a Fellow of the Institute of Electrical and Electronic Engineers cited "for contributions to the computer aided engineering of non-linear microwave and millimeter-wave circuits."